Experimental observation of the splitting of single photons by a beam splitter

J. D. Franson
Applied Physics Laboratory, The Johns Hopkins University, Laurel, Maryland 20723
(Received 23 December 1996)

It was recently predicted that any metallic beam splitter must have a small probability of splitting a single photon into a pair of secondary photons, conserving energy in the process. This nonlinear effect is a consequence of the quantization of the field and is somewhat analogous to other nonlinear effects in QED. The splitting of single photons by a metallic beam splitter has now been observed experimentally and is in good agreement with the theoretical predictions. [S1050-2947(97)07709-3]

PACS number(s): 12.20.Fv, 03.65.Bz, 42.50.Ct

I. INTRODUCTION

A beam splitter is one of the simplest and most widely used components in optics. From a classical viewpoint, these devices ''split'' an incident beam into two outgoing beams, while at the single-photon level it is the probability amplitude that is ''split'' and not the photons themselves [1,2]. The author recently predicted [3], however, that any metallic beam splitter must have a small probability of actually splitting an incident photon into two secondary photons, conserving energy in the process. This nonlinear behavior is a consequence of the quantization of the electromagnetic field and involves the creation and annihilation of electron-positron pairs, which makes it somewhat analogous to other nonlinear effects in QED, such as the scattering of one photon by another [4].

This paper describes an experimental observation of the splitting of single photons by a conventional metallic beam splitter. The rate at which these events were observed is consistent with the earlier theoretical predictions for a simple metal. A number of alternative mechanisms for the observed pairs of secondary photons have been considered, but none appear to be consistent with the experimental observations. To the author's knowledge, this is the first experimental observation of the splitting of photons by a beam splitter, regardless of the mechanism responsible for the secondary photons.

II. THEORY

In the case of a simple metal, a beam splitter can be modeled reasonably well as a large number of free electrons [5] confined to a three-dimensional potential well. To lowest order in perturbation theory, the splitting of single photons is then due to the presence of the nonlinear $\mathbf{A}^2$ term in the nonrelativistic Hamiltonian, where $\mathbf{A}$ is the vector potential operator. An incident photon can be absorbed by the $\mathbf{j}\cdot\mathbf{A}$ term in the Hamiltonian, after which the $\mathbf{A}^2$ term in the Hamiltonian can simultaneously emit a pair of secondary photons. In addition to this basic process, there are five similar processes leading to the same final state, as described in Ref. [3].

The probability P_2 of splitting a photon can be put into a simple form when normalized to the probability P_1 that it will simply be reflected in the usual way:

$$R=\frac{P_2}{P_1}=\frac{2^{7/2}\alpha}{\pi^6}\left(\frac{\lambda_c}{\lambda_0}\right)^2 c_I. \tag{1}$$

Here α is the fine structure constant, λ_c is the Compton wavelength of the electron, and λ_0 is the wavelength of the incident photon with angular frequency ω_0. The dimensionless constant c_I is given by

$$\begin{aligned} c_I=\sum_{\hat{\epsilon}_1,\hat{\epsilon}_2}\int_0^{\sqrt{2}} d\Delta p_z \int_0^{\pi} d\theta' \int_0^{2\pi} d\phi' \frac{p_1\sin\theta'}{(1-p_f\cos\theta')} \\ \times\left[\frac{(\hat{\boldsymbol{\epsilon}}_1\cdot\hat{\boldsymbol{\epsilon}}_2)\hat{\boldsymbol{\epsilon}}_0\cdot\left(\mathbf{p}_{1z}+\mathbf{p}_{2z}+\frac{\pi^2}{8}\mathbf{p}_{0\perp}\right)}{p_0}\right. \\ +\frac{(\hat{\boldsymbol{\epsilon}}_1\cdot\hat{\boldsymbol{\epsilon}}_0)\hat{\boldsymbol{\epsilon}}_2\cdot\left(\mathbf{p}_{0z}-\mathbf{p}_{1z}+\frac{\pi^2}{8}\mathbf{p}_{2\perp}\right)}{p_2} \\ \left.+\frac{(\hat{\boldsymbol{\epsilon}}_2\cdot\hat{\boldsymbol{\epsilon}}_0)\hat{\boldsymbol{\epsilon}}_1\cdot\left(\mathbf{p}_{0z}-\mathbf{p}_{2z}+\frac{\pi^2}{8}\mathbf{p}_{1\perp}\right)}{p_1}\right]^2, \end{aligned} \tag{2}$$

where $\mathbf{p}_0$, $\mathbf{p}_1$, and $\mathbf{p}_2$ are the wave vectors of the initial photon and the two secondary photons. Equation (1) neglects scattering and is valid in the limit of long wavelengths. It can be seen that the ratio R is independent of any properties of the material comprising the beam splitter in this limit, including its thickness, which illustrates the fundamental nature of these effects.

Although the nonlinear nature of the $\mathbf{A}^2$ term seems apparent, the Hamiltonian in relativistic QED does not explicitly contain such a term. It can shown that the $\mathbf{A}^2$ term arises in the nonrelativistic limit of QED as a result of the production of virtual electron-positron pairs. Thus the splitting of photons at a metallic beam splitter is somewhat analogous to other nonlinear effects [4] in QED (which also involve the production of virtual pairs), most of which have not been observed experimentally.

A gauge transformation [6] can be used to express the Hamiltonian in the form of a multipole expansion, in which case the $\mathbf{A}^2$ term no longer explicitly appears in the Hamiltonian and the effects described above correspond instead to

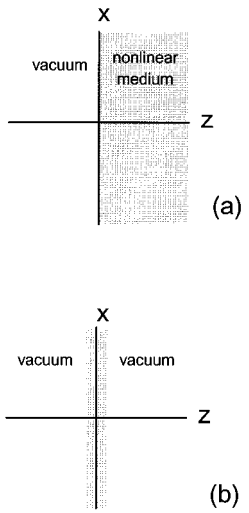

FIG. 1. Difference in inversion symmetries of a thin film and the surface of a bulk nonlinear material. (a) At the surface of a bulk nonlinear material, there is no inversion symmetry and the electronic eigenstates need not have well-defined parity. (b) The addition of a second interface to form a thin film restores the inversion symmetry and the electronic eigenstates have well-defined parity, which rules out the possibility of three dipole transitions returning to the initial electronic state. The presence of a glass substrate does not affect the parity of the electronic states and can be ignored [12].

higher multipole terms. The results are, of course, the same in either gauge, but their interpretation may appear to be somewhat different, which should be kept in mind when comparing the calculations of Ref. [3] with other approaches in nonlinear optics.

In addition to the second-order process involving the $\mathbf{A}^2$ term, the same effect could also be obtained in principle via the $\mathbf{j}\cdot\mathbf{A}$ term alone in third order. Three dipole transitions of that kind are usually responsible for parametric down-conversion [7–9] or second-harmonic generation [10] in nonlinear materials but they cannot contribute here because of parity considerations [3]. Three dipole transitions would have to bring the system back to its initial electronic state in order to maintain coherence and phase matching. That is not possible if the electronic states have well-defined parity (since the dipole matrix elements are zero between states of the same parity) and some source of asymmetry is required. In a bulk material, this process is possible only if the crystal structure is anisotropic, as is the case for all of the $\chi^{(2)}$nonlinear crystals. At the surface of a bulk material, however, the inversion symmetry is broken as illustrated in Fig. 1(a) and it is well known [10,11] that the usual three-dipole transition can produce second-harmonic generation even if the material is isotropic. As can be seen from Fig. 1(b), the addition of a second surface to create a thin film has the effect of restoring the inversion symmetry [12]. In that case, the electronic states once again have well-defined parity and three dipole transitions are not allowed. The calculations of Ref. [3] did not include the possibility of any additional asymmetries associated with the crystalline structure of the material, but the thin films used in this experiment were amorphous.

In principle, the $\mathbf{j}\cdot\mathbf{A}$ term could still contribute in third order, but with reduced magnitude, by means of nondipole transitions. Cancellation between the various diagrams of Ref. [3] causes the nondipole contribution from the $\mathbf{j}\cdot\mathbf{A}$ term to be negligible compared to the $\mathbf{A}^2$ term, provided that the beam splitter is sufficiently thin that perturbation theory can be used to describe the effect as a scattering process. This result may not be too surprising, since it is well-known [13] that the scattering of light by free electrons is dominated by the $\mathbf{A}^2$ term. These calculations correspond to an idealized situation in which there is no dissipation and the electronic wave functions are standing waves with planar boundaries, which does not include any possible effects of surface roughness; this is very different from the conditions considered in earlier free-electron analyses [14,15] of nonlinear effects at the surface of a bulk material, as in Fig. 1(a). More detailed theoretical calculations, including the effects of surface roughness, dissipation, and band structure, would be desirable.

Nonlinear optical effects are often described in terms of an expansion of the polarization $\mathbf{P}$ of the form

$$\mathbf{P}=\chi^{(1)}\cdot\mathbf{E}+x^{(2)}:\mathbf{EE}+\cdots, \tag{3}$$

where $\chi^{(1)}$ and $\chi^{(2)}$ are nonlinear susceptibility coefficients and $\mathbf{E}$ is the electric field. Spontaneous parametric down-conversion or the photon splitting observed in this experiment can be derived from this formalism only if the effects of vacuum fluctuations are included in an *ad hoc* manner, as is discussed in the Appendix. Nevertheless, it may be useful to characterize the photon splitting rate observed here in terms of an effective $\chi^{(2)}$ coefficient, in which case the photon splitting can be viewed as being the result of the nonlinear susceptibility of free electrons confined to a potential well. The usual theory of spontaneous parametric down-conversion can be used to calculate [7–9] the signal photon power ΔP_1 emitted into a solid angle $\Delta\Omega$ and an angular frequency interval $\Delta\omega_1$:

$$\Delta P_1=\frac{4P_0\hbar(\chi^{(2)})^2 n_1\nu_2\omega_1^4\omega_2}{n_0 n_2|\nu_{2z}|c^5}\,\frac{\sin^2(\frac{1}{2}\Delta kL)}{(\frac{1}{2}\Delta k)^2}\,\Delta\Omega\Delta\omega_1. \tag{4}$$

Here P_0 is the incident pump power; ω_1, ω_2, and ω_0 are the angular frequencies of the signal, idler, and pump photons; n_1, n_2, and n_0 are the corresponding indices of refraction; ν_2 is the group velocity of the idler photon; Δk is the wave number mismatch in the direction of propagation; and L is the thickness of the nonlinear medium. Equation (4) can then be used to relate the observed rate of photon splitting to an equivalent nonlinear susceptibility.

One might ask whether or not there is a classical interpretation of these effects. The right-hand side of Eq. (1) is proportional to Planck's constant, so that the theoretical predictions are clearly quantum mechanical in origin. The derivation of Eq. (4) requires the use of vacuum fluctuations, which again shows that these effects are inherently quantum mechanical. More generally, any nonlinear terms that may be present in a classical theory must become negligibly small in the limit of low intensities and induced currents [3]. For example, at low intensities a classical treatment [16] of the electrons in a metallic beam splitter would give Ohm's law with a complex conductivity, which is a linear equation that

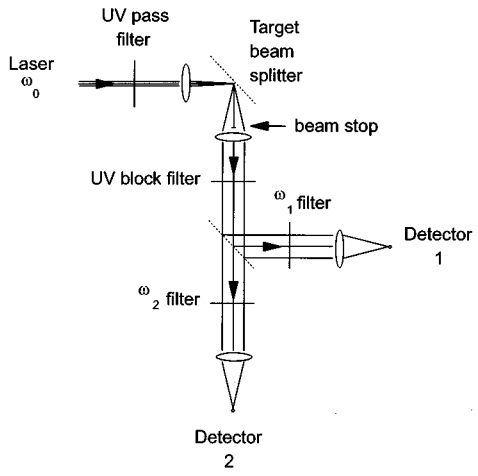

FIG. 2. Sketch of the experimental apparatus. The diameter of the incident laser beam is not drawn to scale, and is sufficiently small that most of the UV photons are blocked by the beam stop.

cannot produce any harmonics or subharmonics. In contrast, the nonlinear results of Eq. (1) are valid for arbitrarily low intensities, which further illustrates their nonclassical nature [17]. At high intensities, the classical theory of a free-electron gas or plasma can produce higher harmonics due to the Lorentz force and other effects, but no subharmonics are predicted [18,19]. This is a general feature of any classical theory when the induced fields are much smaller than the incident field, as is discussed in the Appendix, and that condition is well satisfied in this experiment. These fundamental differences between the classical and quantum predictions can be interpreted as being due to the lack of vacuum fluctuations in classical electromagnetism.

III. EXPERIMENTAL APPROACH

The numerical value of the ratio R is approximately 0.96×10^{-13} at a typical incident wavelength of 351 nm. When combined with the other experimental factors described below, the expected rate of detection of photon-splitting events was only a few events per day. This is relatively low for an optical experiment, where the detector noise is typically 100 Hz or more. As a result, the experimental design included several features intended to minimize the accidental counting rate due to fluorescence and detector noise, as illustrated in Fig. 2. Since the secondary photons are emitted simultaneously, a narrow ($\sim$350 ps) coincidence window was used to reject accidental events. A second beam splitter allowed one photon to reach each of the two detectors. Energy conservation required that

$$\omega_1+\omega_2=\omega_0, \tag{5}$$

where ω_1 and ω_2 are the angular frequencies of the two secondary photons. Two narrow-band interference filters at frequencies ω_1 and ω_2 were used to reject any photon pairs whose total energy did not equal that of the incident photon. Both of these filters were centered on 702 nm with a full width at half maximum of 10 nm, while the incident photons were from an argon-ion laser at 351 nm.

The accidental counting rate due to fluorescence was further reduced by lowering the intensity I of the incident laser beam, since the accidental rate was proportional to I^2 while the photon splitting rate was expected to be proportional to I itself from Eq. (1). On the other hand, accidental events due to detector noise became increasingly significant as the intensity was reduced. The best compromise between these two sources of noise (the highest signal-to-noise ratio) was achieved for an incident intensity of 1.7 mW, which was therefore used for all of the measurements. As a result, it was not possible to verify explicitly the nonclassical intensity dependence of Eq. (1) over a range of intensities.

The two detectors were custom-made silicon avalanche photodiodes (modified EG&G SPCM 100 modules) with detection efficiencies of 70% and average dark counts of 60 Hz. This combination of high efficiency and low noise was achieved in these detectors by limiting their active element to a 100-μm-diameter area. The incident photons were therefore focused onto a small ($\sim$30 μm) spot on the surface of the beam splitter which was then imaged onto the detectors, as illustrated in Fig. 2. This placed a further constraint on the incident laser power, since a focused ultraviolet beam of sufficiently high power would damage the beam splitter. It was found that a small but measurable change in the properties of the beam splitter occurred after roughly one week of exposure. The laser beam was therefore refocused onto a different location every two days. The beam splitter was mounted on a three-axis micropositioner under computer control, which greatly facilitated the focusing process.

The small effective area of the detectors and their large distance ($\sim$1.5 m) from the rest of the apparatus made the coincidence counting rate very insensitive to any photon pairs that may have been created outside of the focal region on the target beam splitter. This effectively eliminated any events due to fluorescence in the lenses or the second beam splitter. The incident ultraviolet photons were prevented from reaching the detectors by a small beam stop (mirror) and appropriate filters, as shown in Fig. 2. The possibility of spurious events at zero time delay due to correlated noise pulses, such as electrical spikes or cosmic ray showers, was also reduced by positioning one of the two detectors further from the beam splitter than the other, and adjusting the time delays accordingly, which shifted any spurious events of that kind away from the region of zero time delay [20].

Unlike the situation for parametric down-conversion [7–9] in a crystal, momentum is not conserved in the direction perpendicular to the beam splitter and secondary photons are emitted into all directions. A fraction of the secondary photons was collected by an achromatic lens with a diameter of 2.54 cm and a focal length of 60 mm. This lens also collimated the outgoing beam, as required by the narrow-band filters.

Pulses from the two detectors were analyzed using a custom-made set of discriminators followed by a time-to-amplitude converter and an analog-to-digital converter. The differences in arrival times of the photon pairs were automatically recorded by a small computer, which allowed the data to be binned as desired at a later time.

Several different types of metallic beam splitters were investigated in an attempt to minimize the accidental counting rate due to fluorescence. It was found that a commercially

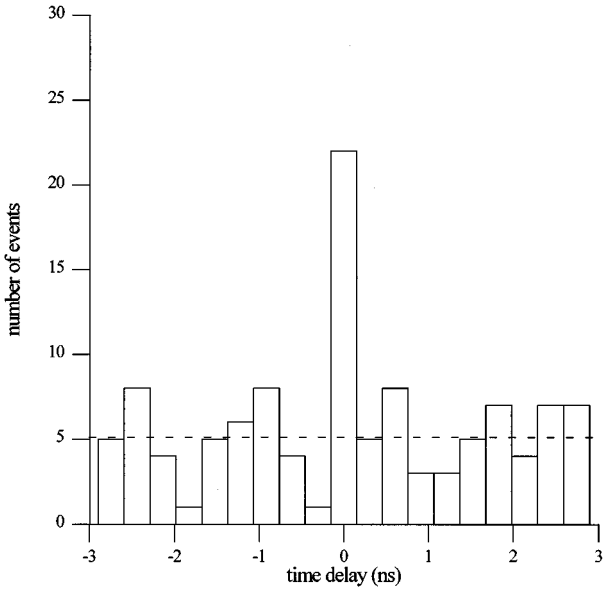

FIG. 3. Experimental data obtained with the filters adjusted to accept energy-conserving events.

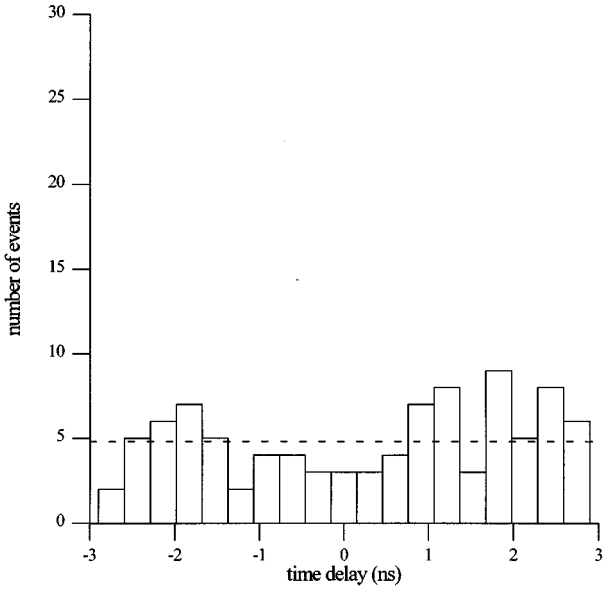

FIG. 4. Control data obtained with the filters adjusted to reject energy-conserving events.

available inconel beam splitter on a fused silica substrate (Oriel model 44941) produced the smallest amount of fluorescence. All of the results presented below were obtained from that type of beam splitter, since the background counting rate was too high for the other types, which ruled out the possibility of a systematic study of these effects in different materials.

In addition to the test data collected as described above, control data were also collected by rotating one of the two interference filters through a small angle, which changed its center wavelength from 702 to 682 nm. With this change in filter wavelength, photon pairs that conserved energy in accordance with Eq. (5) could no longer arrive at both of the detectors. This provided a convenient way to rule out the possibility of various spurious effects [20], since a peak in the test data with no peak in the control data would provide strong evidence that the test data events were due to energy-conserving photons emitted at the same time from within the beam splitter. Test data were collected over a time interval of approximately one week, after which a control run of the same length was made. This process was then repeated for approximately 800 h of total data collection.

IV. EXPERIMENTAL RESULTS

A histogram of the combined test data is shown in Fig. 3, which is a plot of the total number of events obtained as a function of the time delay between the detection of the two photons (corrected for the difference in the distances to the two detectors). An obvious peak can be seen at zero delay time. A fit to the background counting rate is represented by the dashed line and is in good agreement with the expected accidental counting rate for the observed singles rates in the two detectors. The peak in the data at zero delay time is approximately eight standard deviations larger than the background.

Figure 4 shows the corresponding control data obtained with one of the two filters tilt-tuned to eliminate all energy-conserving events. The counting rate at zero time delay was consistent with the accidental counting rate for these control runs, which provided strong evidence that the actual data of Fig. 3 corresponded to coincident pairs of secondary photons.

In order to compare the experimental results with the theory, the integral in Eq. (2) had to be modified to include the effects of experimental factors such as the limited solid angles, the detector efficiencies, and the transmission bandwidth of the filters. This was conveniently done using the Monte Carlo technique, which simulated the trajectories of a large number of pairs of photons, while rejecting those that would not have been detected. The results of this calculation gave an expected counting rate of 2.7 coincident events per day.

The peak in Fig. 3 corresponds to a photon splitting rate of 1.04 ± 0.29 events per day above the background, which is a factor of 2.6 less than that predicted by Eq. (1). Part of this discrepancy could be due to unknown experimental error (for example, in the focusing of the photons onto the detectors), but it seems unlikely that systematic error could account for a discrepancy of this magnitude. Perhaps the most likely explanation is the neglect of scattering in the calculations of Ref. [3], since thin metallic films generally have relatively short electron mean free paths. In particular, the inconel beam splitters used in this experiment reflected approximately 32% of the incident light, transmitted 32%, and absorbed the remaining 36%, so that the neglect of scattering and other dissipative processes is at best a rough approximation. More detailed theoretical calculations including dissipative effects would be desirable but would be much more complex than those of Ref. [3].

V. DISCUSSION

It seems reasonably certain that the peak in Fig. 3 is due to the splitting of single photons by the beam splitter, and the

observed coincidence counting rates are in reasonable agreement with those predicted from the theory of Ref. [3]. Thus the most straightforward interpretation of these results is that the observed photon splitting events are due to the $\mathbf{A}^2$ term associated with free electrons confined to the thin film. But the possibility that these secondary photons may have been produced by some other mechanism must also be considered.

Any alternative interpretation involving some mechanism other than the $\mathbf{A}^2$ term would have to be based on an assumed inadequacy of the free-electron model of Ref. [3], such as the fact that it does not include interactions between the electrons. It should be emphasized once again that Ref. [3] properly included all asymmetries associated with the surfaces of the thin film, and that the usual surface effects [10,11] based on three dipole transitions cannot occur for this geometry due to parity considerations. The contribution from the $\mathbf{j}\cdot\mathbf{A}$ term in third order due to nondipole transitions is also expected to be negligible.

A number of alternative mechanisms for the photon splitting have been suggested, but none appear to be consistent with the observed results. As discussed previously and in the Appendix, classical models can produce higher harmonics but are unlikely sources for the subharmonics observed here. Atomic fluorescence would not be consistent with the experimental results unless there was a cascade of atomic energy levels whose transition energies were both exactly equal to half of the incident photon energy, which seems sufficiently unlikely to be of any serious concern. Collective modes, including plasma oscillations [11,18,19] and various surface plasma effects [21], typically involve the transfer of energy to those modes [11] and would not be expected to produce a pair of energy-conserving photons as observed.

Perhaps the most plausible alternative source of the observed photon pairs was contamination of the surface of the metallic film with a thin, nonisotropic layer of atoms or molecules possessing an inherent $\chi^{(2)}$ nonlinearlity, which could have produced photon pairs by parametric down-conversion [7–9] in the usual way. A rough estimate of the likely effects of such a layer of contamination can be obtained by using Eq. (4) to calculate the expected coincidence rate from a thin (1 Å) layer of material with a nonlinear susceptibility equal to that of $LiIO_3$, for example, which is commonly used for parametric down-conversion because of its large value of $\chi^{(2)}$ (4.4 pm/V). An upper bound on the expected coincidence rate can be obtained by assuming that an idler photon is emitted into the solid angle of the detectors whenever a signal photon has been detected, which gives a maximum coincidence rate of 0.0028 events per day for the detection efficiencies and solid angles of this experiment. This is nearly three orders of magnitude smaller than the observed coincidence rate, which strongly suggests that a thin layer of contamination could not be responsible for the observed experimental results. In addition, the fundamental $\mathbf{A}^2$ mechanism described above provides a lower limit on the rate of photon splitting, and any significant contribution from contamination (or any other spurious mechanism) should have produced a larger photon splitting rate, whereas the observed photon splitting rate was actually somewhat less than that expected from the $\mathbf{A}^2$ term alone.

Equation (4) can also be used to estimate the effective $\chi^{(2)}$ for the thin film itself based on the observed coincidence rate and film thickness of 90 Å. This gives $\chi^{(2)}_{\text{eff}}\sim 0.9$ pm/V, which is comparable to that of some commonly used nonlinear crystals. This value of $\chi^{(2)}$ is consistent with what would be expected from the free-electron model of Ref. [3], where the nonlinearity is due to the $\mathbf{A}^2$ term in the Hamiltonian.

VI. SUMMARY AND CONCLUSIONS

The splitting of single photons by a metallic beam splitter has been experimentally observed. The rate at which these events occurred was somewhat less than was predicted by a free-electron model, presumably due to the neglect of scattering in the calculations. A number of other possible mechanisms for the production of the observed secondary photons were also considered, but do not appear to be consistent with the observed experimental results. Although these results can be interpreted in terms of an effective $\chi^{(2)}$ nonlinearity (and vacuum fluctuations), the usual dipole transitions are forbidden by parity considerations. Contributions from the $\mathbf{j}\cdot\mathbf{A}$ term in third order due to nondipole transitions are also expected to be negligible compared to the $\mathbf{A}^2$ term, in which case these nonlinear effects are fundamental in nature and somewhat analogous to other nonlinear effects in QED, such as the scattering of one photon by another. An ordinary beam splitter, which forms the basic building block of so many fundamental experiments in quantum optics, can be seen to be the source of complex phenomena of its own.

ACKNOWLEDGMENTS

The author is grateful to D. N. Klyshko and T. B. Pittman for valuable discussions. This work was supported by the Office of Naval Research.

APPENDIX

Although the right-hand side of Eq. (1) is proportional to Planck's constant, it has been suggested nevertheless that some (unspecified) classical model might be able to account for the experimental data, since the measurements could not be performed in the limit of arbitrarily small intensities where any classical nonlinearities clearly vanish. It will be shown in this appendix that no classical model can produce subharmonic frequencies if the induced fields are much smaller than the incident field, which is the case in this experiment.

The desired result can be easily derived if one is willing to assume only that the classical theory is deterministic in the sense that the output field $\mathbf{E}_{\text{out}}(t)$ can be calculated given the input field $\mathbf{E}_{\text{in}}(t)$, as in Eq. (3). If the induced fields are sufficiently weak compared to the incident field, then a well-known iterative technique [18,19] can be used to explicitly solve Eq. (3) for $\mathbf{E}_{\text{out}}(t)$. The input field will be assumed to have the form $\mathbf{E}_{\text{in}}=\sin(\omega_0 t)$. The corresponding output field can then be represented by a Fourier expansion of the form

$$\mathbf{E}_{\text{out}}(t)=c_0\sin(\omega_0 t+\phi_0)+c_{1/2}\sin(\omega_0 t/2+\phi_{1/2})+\cdots, \tag{A1}$$

where the c's and ϕ's are coefficients determined by the solution to Eq. (3). Only the subharmonic at $\omega_0/2$ has been included in Eq. (A1), but a similar proof can be given for any

other subharmonic. Now consider a change of variables to a time $t'=t+\tau_0$ where τ_0 is the period of the input field. The output field becomes

$$\mathbf{E}_{\rm out}(t')=c_0\sin(\omega_0 t'+\phi_0)-c_{1/2}\sin(\omega_0 t'/2+\phi_{1/2})+\cdots. \tag{A2}$$

Since $\mathbf{E}_{\rm in}(t')=\mathbf{E}_{\rm in}(t)$, the solution to Eq. (3) will be the same in both cases, which gives $\mathbf{E}_{\rm out}(t')=\mathbf{E}_{\rm out}(t)$ as well. Setting the right-hand sides of Eqs. (A1) and (A2) equal to each other gives $c_{1/2}=0$, which shows that no subharmonics can be generated. Higher harmonics are not precluded, of course, and can appear in classical models even for induced fields of relatively low intensity.

The quantum theory often predicts subharmonic fields whose phases are totally unpredictable and not determined by the input field. There spontaneous emission can be viewed, at least intuitively, as being due to vacuum fluctuations which have no classical analogy. In discussing the onset of lasing, Bloembergen [18] states that ''a proper description . . . would be possible only with quantum mechanics, since spontaneous emission must be invoked, which might be considered in a nonrigorous fashion as noise from zero point vibrations.'' The dependence of effects of this kind on the magnitude of the vacuum fluctuations can be seen from the fact that Eq. (1) is proportional to Planck's constant.

The above argument is no longer valid if the induced fields are so large that the iterative procedure does not converge. In that case there may be multiple solutions and a strong sensitivity to noise, so that the output cannot be viewed as a deterministic result of the input. This can occur, for example, if a high-gain system is enclosed in a resonant cavity where the induced fields can grow to very large intensities, as in a laser. That is not the situation here.

[1] J. F. Clauser, Phys. Rev. D **9**, 853 (1974).

[2] R. A. Campos, B. E. A. Saleh, and M. C. Teich, Phys. Rev. A **40**, 1371 (1989).

[3] J. D. Franson, Phys. Rev. A **53**, 3756 (1996).

[4] M. Delbruck, Z. Phys. **84**, 144 (1933); R. Karplus and M. Neuman, Phys. Rev. **83**, 776 (1951).

[5] C. Kittel, *Introduction to Solid State Physics* (Wiley, New York, 1968).

[6] C. Cohen-Tannoudji, J. Dupont-Roc, and G. Grynberg, *Photons and Atoms: An Introduction to Quantum Electrodynamics* (Wiley, New York, 1989).

[7] D. N. Klyshko, *Photons and Nonlinear Optics* (Gordon and Breach, New York, 1988).

[8] D. C. Burnham and D. L. Weinberg, Phys. Rev. Lett. **25**, 84 (1970).

[9] D. A. Kleinman, Phys. Rev. **174**, 1027 (1968).

[10] C. C. Wang and E. L. Baardsen, Phys. Rev. **185**, 1079 (1969); J. E. Sipe, D. J. Moss, and H. M. van Driel, Phys. Rev. B **35**, 1129 (1987).

[11] Y. R. Shen, *The Principles of Nonlinear Optics* (Wiley, New York, 1984).

[12] The presence of a glass substrate on one side of the metallic beam splitter does not affect the symmetry considerations since it is only the parity of the electronic eigenstates that matters, and that is unaffected by the glass substrate. Both surfaces of the beam splitter are equally important for a thin film, since they set the boundary conditions for the electronic wave functions in the free-electron limit. In Fig. 1(a), the thickness of the nonlinear medium is assumed to be much larger than the wavelength of the incident light and the scattering length of the electrons, while the opposite limit holds for the thin beam splitter of Fig. 1(b).

[13] G. Baym, *Lectures on Quantum Mechanics* (Benjamin, Reading, MA, 1969).

[14] J. Rudnick and E. A. Stern, Phys. Rev. B **4**, 4274 (1971).

[15] A. Liebsch, Phys. Rev. Lett **61**, 1233 (1988); A. Liebsch and W. L. Schaich, Phys. Rev. B **40**, 5401 (1989).

[16] M. Born and E. Wolf, *Principles of Optics* (Pergamon, New York, 1980).

[17] J. D. Franson, Phys. Rev. A **45**, 8074 (1992).

[18] N. Bloembergen, *Nonlinear Optics*, 4th ed. (World Scientific, River Edge, NJ, 1996).

[19] R. F. Whitmer and E. B. Barrett, Phys. Rev. **121**, 661 (1961); **125**, 1478 (1962).

[20] For example, it is well known that the detection of a single photon by an avalanche photodiode can produce a large number of other photons as energy is dissipated in the device. But these photons have a broad spectral distribution and would have produced the same effect in the control data of Fig. 4, which was not observed. In addition, the optical path separation between the two detectors was 1.6 m, which would have displaced any such spurious coincidence peak by 5 ns from the observed peak at zero time delay.

[21] For a recent discussion, see J. A. Maytorena, W. L. Mochan, and B. S. Mendoza, Phys. Rev. B **51**, 2556 (1995).